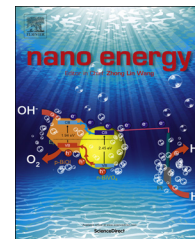Available online at www.sciencedirect.com

ScienceDirect

journal homepage: www.elsevier.com/locate/nanoenergy

SHORT COMMUNICATION

Nanoconfined antimony in sulfur and nitrogen co-doped three-dimensionally (3D) interconnected macroporous carbon for high-performance sodium-ion batteries

Chenglong Yang[a], Weihan Li[a], Zhenzhong Yang[c], Lin Gu[c], Yan Yu[a,b,*]

[a]Key Laboratory of Materials for Energy Conversion, Chinese Academy of Sciences, Department of Chemistry and Materials Science, University of Science and Technology of China, Hefei, Anhui 230026, China
[b]State Key Laboratory of Fire Science, University of Science and Technology of China, Hefei, Anhui 230026, China
[c]Beijing National Laboratory for Condensed Matter Physics, The Institute of Physics, Chinese Academy of Sciences, Beijing 100190, China

Abstract
The Sb encapsulated in S and N co-doped three-dimensionally (3D) interconnected macroporous carbon composite (denoted as Sb@S,N-3DPC) has been fabricated by using silica opals as hard template following a carbonization process. The structural and morphological characterizations reveal the uniform 3D-network structure with the Sb nanoparticles embedded homogeneously in the carbon spherical shell. The Sb@S,N-3DPC electrode shows a high reversible capacity of 482 mAh g^{-1} at 100 mA g^{-1}, displaying good capacity stability ($\sim$93% of the initial discharge capacity after 500 cycles at 100 mA g^{-1}). The electrode displays superior rate capability and ultralong cyclability (255 mAh g^{-1} at 2 Ag^{-1} after 2000 cycles) and also reveals a good rate capability that maintains 160 mAh g^{-1} at 5 Ag^{-1}. The excellent electrochemical performance of the Sb@S,N-3DPC is attributed to the 3D-porous carbon network structure and uniform distribution of Sb nanoparticles in carbon matrix, enhancing the conductivity, holding the structure integrity, and thus improving the cycling performance of the anode material. In addition, sulfur and nitrogen co-doping introduced more defects and active sites to the carbon framework, thereby improving the interfacial adsorption and electrochemical behaviors.
© 2015 Elsevier Ltd. All rights reserved.

*Corresponding author at: Key Laboratory of Materials for Energy Conversion, Chinese Academy of Sciences, Department of Chemistry and Materials Science and State Key Laboratory of Fire Science, University of Science and Technology of China, Hefei, Anhui 230026, China.
E-mail address: yanyumse@ustc.edu.cn (Y. Yu).

Introduction

While much effort has been devoted to the development of high performance lithium-ion batteries (LIBs) for renewal energy storage applications [1-4], the sodium-ion battery (NIBs) attracted increasing attention because of the abundant resource of sodium and decent energy densities [5-7]. However, compared with LIBs, NIBs inevitably experience two critical problems: (i) the radius of Na (0.98 Å) is much larger than that of Li (0.69 Å), which leads to a poorer kinetic performance and a lower diffusion coefficient of Na^+ [8,9]. (ii) The huge volumetric expansion and contraction associated with the larger Na ions insertion/extraction of the electrode materials cause the severe structure degradation, finally leading to rapid capacity fading of the battery [9,10]. Thus, the research for suitable electrode materials for NIBs remains challenging [11]. Due to the formation of dendritic Na during cycling, pure Na metal is not an appropriate anode material for NIBs, which gives rise to a safety issue. Many pioneering works have reported some anode material candidates for NIBs, including Ti-based materials, carbonaceous materials, and alloy-based materials [12-16]. Among them, alloy-based materials (i.e. Sn, Sb, Ge, Pb) are also of considerable interests as high capacity anodes for NIBs because of their high theoretical specific capacities and low reaction potential [17-22]. Recently, Sb has been demonstrated as one of the most promising alternatives due to its high theoretical capacity (660 mAh g^{-1}) [23,24]. However, the volume-expansion-caused pulverization of the Sb particles in the electrode, which results in loss of contact between the electroactive particles and consequently severe capacity fade [25].

Various efforts have been made to overcome these issues and enhance the electrochemical performance of Sb-based anode materials for NIBs [16-24,26]. Among these approaches, downsizing of Sb particles to nanoscale level and control of morphology of the Sb particles have been demonstrated as effective ways to enhance cycling stability and rate capability [22,21,27]. Another promising strategy is dispersion of the Sb particles in carbon matrix that can act as a stress-buffer during volume expansions, which will improve the electronic and ionic conductivities and also the stability of the anodes [21,28,29]. Among these carbonaceous materials, ordered macroporous carbon with a three-dimensional (3D) interconnected pore structure exhibits high surface area, uniform pore diameter, interconnected porous structure, high volume and shows excellent electrical conductivity and improved lithium storage performance [29-31,32-38]. Besides, the heteroatom (e.g., N, B, S, P) doped and co-doped carbonaceous materials can also help to improve its electrical properties and chemical activity, which is very favorable for energy storage [39,40-43].

Herein, we designed the unique 3D structure: Sb nanoparticles confined in Sulfur (S) and Nitrogen (N) co-doped 3D interconnected macroporous carbon (denoted as Sb@S, N-3DPC) were synthesized by using silica opals as hard template following a carbonization route. When used as anode for NIBs, the Sb@S,N-3DPC shows an ultralong cycle life (480 mAh g^{-1} after 500 cycles at 100 mA g^{-1}), superior rate capability (255 mAh g^{-1} at 2 A g^{-1}) and excellent cycling efficiency.

Result

Scheme 1 illustrates the detailed fabrication process of the Sb@S,N-3DPC anode. Firstly, the silica nanospheres are fabricated by the Stöber method [44]. Then silica nanospheres were mixed with1-allyl-2-thiourea and $SbCl_3$ in deionized water. The hydrochloric was employed to keep the solution acid to control the hydrolysis of $SbCl_3$ [45]. The 1-allyl-2-thiourea can dissolve very well and a solution was formed to facilitate its adsorption onto the silica surface. Afterwards, the sample was dried for overnight. The dried sample was subsequently calcined to get 3D interconnected silica nanospheres coated by carbon. Finally, Sb embedded in the S and N co-doped 3D interconnected macroporous carbon can be obtained after the removal of silica nanospheres by HF.

Figure 1a–d shows the SEM, TEM images, XRD patterns and Raman spectroscopy of the obtained sample (Sb@S,N-3DPC). Figure 1a reveals the morphology of the Sb@S,N-3DPC that displays a 3D ordered structure with spherical voids. It is also seen that the Sb@S,N-3DPC contains quasi-spherical cavities of around 200 nm in diameter. Note that the Sb@S,N-3DPC does not show perfectly pore structure due to some fractures and defects resulting from structural collapses of the silica template during the carbonization or template removal process. The TEM image of Sb@S,N-3DPC (Figure 1b) confirms its 3D interconnected structure constituted by interconnected very thin spherical carbon sheets. As marked in the image the carbon wall thickness is about 5 nm. For comparison, we also prepared Sb-free sample (S and N doped 3D porous carbon, denoted as S,N-3DPC).The Sb-free sample (S,N-3DPC) (Figure S1a,b) shows similar structure with the Sb@S,N-3DPC. Meanwhile, the Sb encapsulated in S,N-codoped carbon sample (porous free sample) was also prepared (denoted as Sb@S,N-C). The Sb@S,N-C displays no 3D structure, massive blocks of 2–10 μm in diameter, as shown in Figure S1c.

The crystalline structure of the Sb@S,N-3DPC was also examined by the XRD pattern. As shown in Figure 1c, all of the XRD peaks of the Sb@S,N-3DPC can be indexed to the hexagonal Sb (JCPDS no. 35-0732), implying that all of the Sb^{3+} was turned to metallic Sb by carbonization process and no impurity exists. Further structural information was measured by Raman spectroscopy (Figure 1d). The two peaks are attributed to the D band (1356 cm^{-1}) and G band (1584 cm^{-1}) of the carbon matrix. The intensity ratio between D and G bands (I_D/I_G) was also calculated since the I_D/I_G could exactly reflect the graphitic degree of the carbon materials. As the value of I_D/I_G is below 1, the carbon of Sb@S,N-3DPC shows partial graphitization. In order to determine the distribution of Sb in the Sb@S,N-3DPC, elemental mapping is performed (Figure 2). Elemental mapping of Sb@S,N-3DPC illustrates a homogeneous distribution of Sb, N, and S atoms in 3DPC.

It is known that for a heteroatom doped carbon, the doping level and the type of bonds formed between dopant and graphitic carbon atoms are important in determining the electrochemistry activity. As shown in Figure 3, the XPS survey spectrum confirms the presence of N and S. The high resolution N_{1s} spectrum (Figure 3a) suggests the presence of two types of N–C bonds such as pyridinic and